JPL PUBLICATION 83-98

Description of Algorithms for Processing Coastal Zone Color Scanner (CZCS) Data

Philip M. Zion

December 15, 1983

National Aeronautics and Space Administration

Jet Propulsion Laboratory
California Institute of Technology
Pasadena, California

JPL PUBLICATION 83-98

Description of Algorithms for Processing Coastal Zone Color Scanner (CZCS) Data

Philip M. Zion

December 15, 1983

NASA
National Aeronautics and
Space Administration

Jet Propulsion Laboratory
California Institute of Technology
Pasadena, California

The research described in this publication was carried out by the Jet Propulsion Laboratory, California Institute of Technology, under contract with the National Aeronautics and Space Administration.

CONTENTS

Figures

Tables

ABSTRACT

The algorithms for processing CZCS data to geophysical units (pigment concentration) are described. This document provides a summary of current public-domain information for processing these data. Calibration, atmospheric correction, and bio-optical algorithms are presented. Three CZCS data-processing implementations are compared.

DESCRIPTION OF ALGORITHMS FOR PROCESSING CZCS DATA

I. INTRODUCTION

This document is a short introduction to the Coastal Zone Color Scanner (CZCS) data and a description of the extant versions of the CZCS algorithm.

The CZCS is a scanning multispectral radiometer with a scan angle of 78 degrees and an instantaneous field of view (IFOV) of 0.0495 degrees. The nominal resolution at 955-km altitude is 825 meters at nadir. To avoid sun glint, the sensor can be tilted forward or backward in 2-degree increments, to a maximum of 20 degrees. The four bands on the CZCS relevant for color work are 20 nm-wide bands centered at 443, 520, 550, and 670 nm. Another band at 700-800 nm is used for detecting land or cloud pixels. A sixth band in the emitted infrared has functioned intermittently during the mission.

The CZCS scans 1968 samples per line. There are two major formats for digital data on magnetic tape, the ZIP format (e.g., Scripps or RSMAS tapes) and NESDIS Level-1 tapes.* This document does not address tape formats or unpacking of data.

The "color algorithm" is threefold (see Figure 1). First, the sensor-apparent total radiances, L_T, are derived from the satellite digital counts using a calibration algorithm. Then the water upwelling radiances, L_W, are derived from the values L_T using an atmospheric correction algorithm. Finally the water upwelling radiances are used to derive the pigment concentration using a "bio-optical" algorithm.

---

*Scripps is the Scripps Institution of Oceanography Satellite Facility. RSMAS is the Rosenstiel School for Marine and Atmospheric Sciences at the University of Miami. NESDIS is the National Environmental Satellite Data and Information Service. All three have various degrees of CZCS data processing capability.

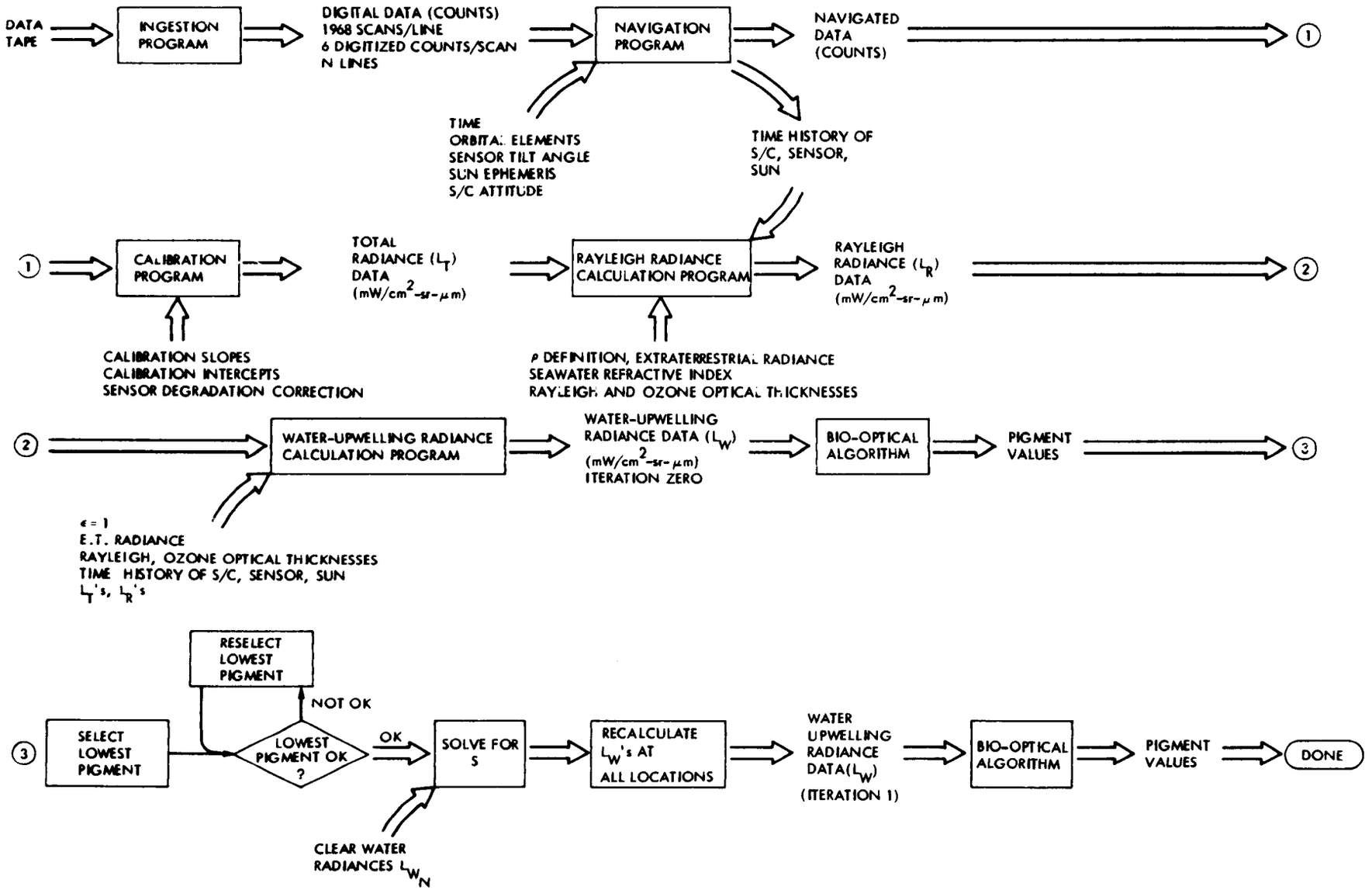

Figure 1. Generic CZCS Algorithm (after Gordon et al., 1983a)

II. CALIBRATION ALGORITHM

During data acquisition, sensor-apparent radiances are digitized for transmission to earth. Calibration equations are used to transform satellite digital counts back to sensor-apparent radiances. Following are the calibration procedures and constants necessary for the conversion. Also included are some other constants needed for later processing.

Sets of calibration coefficients are chosen according to the gain setting of the CZCS (possible range 1-4) for a particular pass. The gain setting must be available to any calibration program.

The equation to convert counts to radiances can be of the form:

$$[A(\lambda)N(\lambda) + B(\lambda)]C'(\lambda) = L_T(\lambda) \quad \text{(the total radiance)}$$

where

N = digital count from the sensor

A = calibration slope

B = calibration intercept

C′ = sensor response correction function, f(C). Determination of C′ depends on the value of C, a correction coefficient. C in turn depends on estimates of the mean extraterrestrial solar radiance $\bar{F}_0$. In short, these three parameters are coupled. Care must be taken to use coherent sets of C′, C, and $\bar{F}_0$. See e.g. Viollier (1982) for other coefficients. The values given here are from Austin (quoted in Gordon et al. (1983a)) and have the advantage of being independent of gain.

λ = wavelength of one of the four visible bands sensed by the CZCS.

It is important to note that the CZCS sensor response has been changing with time (Gordon et al. (1983b)). Current efforts in CZCS calibration therefore define $C'(\lambda)$ as a function of orbit number (time). This sensor degradation correction is the focus of much current activity in the CZCS community.

The coefficients for CZCS parameters A and B in Table 1 were furnished by Mueller (personal communication). The figures for $\bar{F}_o$, m, and the atmospheric optical parameters in Table 2 are from the Goddard Space Flight Center (GSFC) (undated, but probably 1982). All of these are generally undisputed. Figures not universally accepted at the time of this writing are given with references.

Table 1. CZCS Coefficients

	443 nm	520 nm	550 nm	670 nm
A (in mW/cm^2-μm-sr-count)				
Gain 1	0.04452	0.03103	0.02467	0.01136
Gain 2	0.03589	0.02493	0.02015	0.00897
Gain 3	0.02968	0.02032	0.01643	0.00741
Gain 4	0.02113	0.01486	0.01181	0.00535
B (in mW/cm^2-μm-sr)				
Gain 1	0.03963	0.06361	0.07992	0.01136
Gain 2	0.05276	0.08826	0.06247	0.03587
Gain 3	0.02879	0.09752	0.06570	0.02963
Gain 4	0.03359	0.05647	0.04723	0.01604
C (Gordon et al. (1983a), GSFC)				
	1.0688	0.9931	0.9554	1.000
C (Mueller)	1.144	1.033	0.979	1.000

Sensor Degradation Correction Functions, C′:

Gordon et al. (1983b):

$C'(\lambda) = C(\lambda)[a - b(orbit) + c(orbit^2)]$

for λ = 443 nm, a = 1.086, b = 2.46×10^{-5}, c = 5.05×10^{-10} or
a = 1.069, b = 2.32×10^{-5}, c = 5.0×10^{-10}
(see reference)
for λ = 520 nm, a = 1.024, b = 0.59×10^{-5}, c = 0
for λ = 550 nm, a = 1.007, b = 0.28×10^{-5}, c = 0

Mueller:

$C'(\lambda) = C(\lambda)\exp[a(orbit)]$

for λ = 443 nm, a = 2.12×10^{-5}
for λ = 520 nm, a = 1.22×10^{-5}
for λ = 550 nm, a = 0.78×10^{-5}

Table 1. CZCS Coefficients (Continued)

	443 nm	520 nm	550 nm	670 nm
GSFC:				
$C'(\lambda) = C(\lambda)\exp[a(\text{orbit} - 3200)]$ for λ = 443 nm, a = 2.12×10^{-5} for λ = 520 nm, a = 1.22×10^{-5} for λ = 550 nm, a = 0.78×10^{-5}				
$\bar{F}_o$ (in $mW/cm^2-\mu m$)	186.42	185.34	184.76	151.52
m (nominal refractive index of seawater)	1.347	1.342	1.341	1.337

Table 2. Atmospheric Optical Coefficients

	443 nm	520 nm	550 nm	670 nm
τ_R - Rayleigh optical thickness				
< 25° Lat.	0.2329	0.1231	0.0969	0.0444
25°-55° Lat.				
Summer	0.2311	0.1222	0.0962	0.0440
Winter	0.2316	0.1224	0.0964	0.0442
> 55° Lat.				
Summer	0.2300	0.1214	0.0956	0.0438
Winter	0.2303	0.1218	0.0959	0.0439
τ_{oz} - Ozone optical thickness				
< 25° Lat.	0.0066	0.0166	0.0261	0.0158
25°-55° Lat.				
Summer	0.0067	0.0200	0.0323	0.0191
Winter	0.0069	0.0237	0.0390	0.0226
> 55° Lat.				
Summer	0.0068	0.0213	0.0346	0.0202
Winter	0.0071	0.0275	0.0461	0.0264

Notes:

(1) Atmospheric optical parameters are dependent on the time of year and the latitude.

(2) Summer and winter are defined in terms of the local season, the summer/winter boundaries being the spring and autumn equinoxes.

III. ATMOSPHERIC CORRECTION ALGORITHM

The following description is of a color algorithm taken from the Ocean Color Science Working Group (OCSWG) (1982) and Gordon et al. (1983a). Further references for the interested reader may be found in those papers. The detailed provenance of this algorithm is not known; the term "Gordon algorithm" is used as a convention in this document because he is first author of the 1983 paper that sets out clearly in the open literature the steps necessary to implement a generic color algorithm and because he first suggested the general approach (Gordon, 1978). Many of the equations here are taken from Gordon et al. (1983a) and Sturm (1981). Other algorithms do exist, however. The Gordon algorithm is the basis of the GSFC production processing, the RSMAS procedures, and the Mueller procedures. Differences among the RSMAS, Mueller, and GSFC procedures are discussed in Section V, Implementations.

The total radiance apparent to the CZCS may be partitioned into contributions from sun glint (specular reflection from the sea surface), Rayleigh and aerosol backscattering, and the water-leaving radiance. The latter carries information about the pigment concentration of the water. The CZCS mirror is tiltable to avoid glint. The first step in the color algorithm is removing the atmospheric contribution at each wavelength from L_T. Assuming no glint, L_T is given by:

$$L_T(\lambda) = L_R(\lambda) + L_A(\lambda) + t(\lambda)L_W(\lambda) \qquad (1)$$

where

L_R = radiance due to Rayleigh scattering
L_A = radiance due to aerosol scattering
L_W = radiance leaving the water
t = diffuse transmittance to top of the atmosphere

Since calculations of pigment depend on L_W, we shall solve for that term.

We know from physics by way of Gordon et al. (1983a) that:

$$L_A = \frac{\omega_A(\lambda)\tau_A(\lambda)F_o'(\lambda)P_A(\theta,\theta_o,\lambda)}{4\pi} \qquad (2)$$

where

ω_A = single scattering albedo of the aerosol (good approximation to multiple scattering)

τ_A = optical thickness of the aerosol

$P_A(\theta,\theta_o,\lambda)$ = aerosol characterization function, considering the Fresnel reflectance of the interface and the aerosol scattering phase function

F_o' = spacecraft apparent instantaneous extraterrestrial radiance, F_o, corrected for two passes through the ozone layer, a known constant. In practice, F_o values are the mean extraterrestrial radiation values, $\bar{F}_o$, corrected for the CZCS sensor response and the time of year. These $\bar{F}_o$ values must be highly consistent with the sensor calibrations listed in Section II, Calibration Algorithm, and they have been so refined (see Gordon (1981) for discussion of F_o determination). The F_o' values are related to $\bar{F}_o$ by:

$$F_o = \bar{F}_o \left[1 + 0.0167 \cos\left(\frac{2\pi(D-3)}{365}\right)\right]^2$$

$$F_o' = F_o \exp\left[-\tau_{oz}\left(\frac{1}{\cos\theta} + \frac{1}{\cos\theta_o}\right)\right]$$

where

D = Julian day of the year ($1 \leq D \leq 366$)

θ_o = solar zenith from pixel local tangent plane

θ = spacecraft zenith from pixel local tangent plane. Zenith angle measurements must be based on knowledge of sun, spacecraft, and pixel location. Therefore the image must be navigated, i.e., the pixels must be earth-located. (This also applies for azimuth angles that appear later in the algorithm.) A discussion of navigation is beyond the scope of this document. However, in general, navigation depends on knowledge of the orbital characteristics of the spacecraft, accurate time of overpass, and knowledge of spacecraft attitude during overpass. There may be some ambiguity in location description. A specific example of configuration is given in Figures 2 and 3. This configuration is used for Equations 7-10. General illustrations are given in Section V.C, Figures 5-10.

If we assume a constant aerosol "type", i.e., an atmosphere in which the normalized size frequency distribution and the refractive index of the aerosol are independent of horizontal position in the image, then for two wavelengths λ and λ_o, we can define $S(\lambda,\lambda_o)$, the ratio of $L_A(\lambda)$ to $L_A(\lambda_o)$. This ratio $S(\lambda,\lambda_o)$ will be independent of horizontal position in the image, even though $L_A(\lambda)$ and $L_A(\lambda_o)$ may vary.

If we expand the $L_A(\lambda)$ terms in the ratio $S(\lambda,\lambda_o)$ we have:

$$S(\lambda,\lambda_o) = \frac{\omega_A(\lambda)\tau_A(\lambda)F_o'(\lambda)P_A(\theta,\theta_o,\lambda)}{\omega_A(\lambda_o)\tau_A(\lambda_o)F_o'(\lambda_o)P_A(\theta,\theta_o,\lambda_o)} \tag{3}$$

We can name $\varepsilon(\lambda,\lambda_o)$ as the ratio of the products of the aerosol albedo, optical thickness and aerosol function at the respective wavelengths. Of the three unknowns, Gordon et al. (1983a) assume that for aerosol, the albedo and phase function are weak functions of wavelength or viewing angle, and therefore $\varepsilon(\lambda,\lambda_o)$ is determined mostly by the ratios of the aerosol optical thickness at the two wavelengths in question. For a single aerosol type this ratio should be fairly constant, even if the aerosol is not horizontally homogeneous. Then we can state:

$$\frac{L_A(\lambda)}{L_A(\lambda_o)} = S(\lambda,\lambda_o) = \frac{\varepsilon(\lambda,\lambda_o)F_o'(\lambda)}{F_o'(\lambda_o)} \tag{4}$$

where $\varepsilon(\lambda,\lambda_o)$ is assumed constant over the image.

Now substituting into Equation 1, we can solve for the water-leaving radiance $L_W(\lambda)$:

$$t(\lambda)L_W(\lambda) = L_T(\lambda) - L_R(\lambda) - S(\lambda,\lambda_o)\,[L_T(\lambda_o) - L_R(\lambda_o) - t(\lambda_o)L_W(\lambda_o)] \tag{5}$$

The wavelength λ_o is chosen so that $L_W(\lambda_o)$ is minimized. In this way one of the unknowns in Equation 5 is eliminated. In practice, λ_o is the 670 nm CZCS band. Let us consider the terms of this equation left to right. The diffuse transmittance $t(\lambda)$ is given by:

$$t(\lambda) = t_A(\lambda) \exp\left[\frac{-(\frac{\tau_R}{2} + \tau_{oz})}{\cos\theta}\right] \quad (6)$$

where

τ_R = Rayleigh optical thickness, a known constant

τ_{oz} = ozone optical thickness, a known constant

t_A = a function depending on the aerosol optical thickness

In practice, τ_R and τ_{oz} are known. Gordon et al. (1983a) suggest setting $t_A(\lambda)$ to unity since certain assumptions in the algorithm will break down before the aerosol optical thickness starts to affect the diffuse transmittance.

The next known term in Equation 5 is L_T, the total sensed radiance. This is derived from the digitized counts by certain calibration equations (see Section II).

The next known term is the radiance due to Rayleigh scattering, L_R. L_R is given by:

$$L_R(\lambda) = \frac{3t_{oz}(\lambda)\tau_R(\lambda)F_o'(\lambda)}{16\pi\cos\theta}\left([1 + \cos^2\Psi_-] + [1 + \cos^2\Psi_+]\ [\rho(\theta) + \rho(\theta_o)]\right) \quad (7)$$

where

$$\cos\Psi_- = [-\cos\theta\cos\theta_o - \sin\theta\sin\theta_o\cos(\phi_o - \phi - \pi)] \quad (8)$$

$$\cos\Psi_+ = [\cos\theta\cos\theta_o + \sin\theta\sin\theta_o\cos(\phi_o - \phi)] \quad (9)$$

$\rho(x)$ = Fresnel transmittance

$$= 1 - [2m(\lambda)yz]\cos x \qquad (x = \theta \text{ or } \theta_o) \quad (10)$$

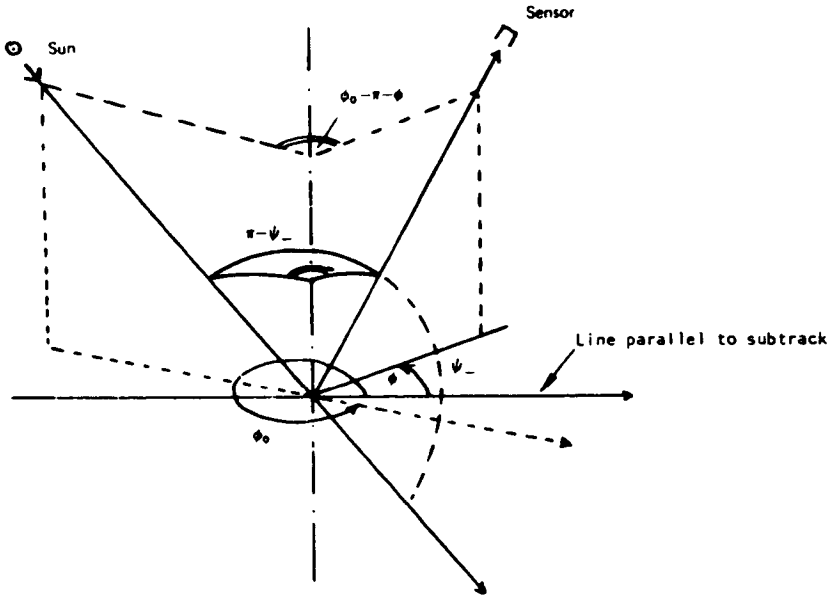

Figure 2. Angular Configuration Used for the Derivation of Ψ_- (Equation 8) (from Sturm, 1981)

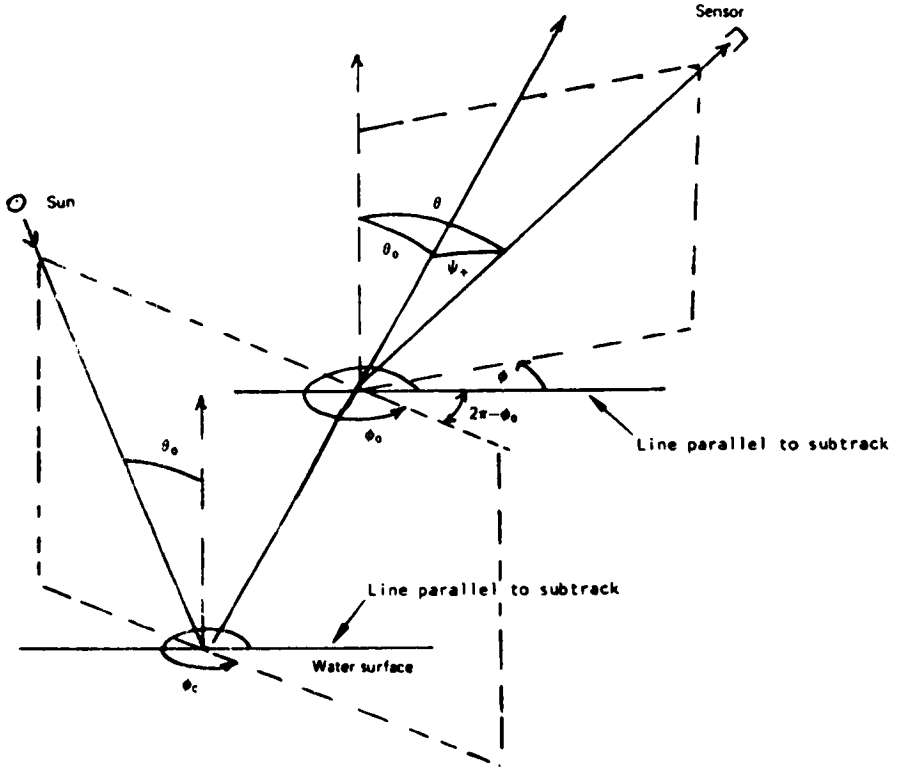

Figure 3. Angular Configuration Used for the Derivation of Ψ_+ (Equation 9) (from Sturm, 1981)

$t_{oz}(\lambda)$ = ozone transmittance to top of atmosphere

$$= \exp\ -\tau_{oz}(\lambda)\ \left[\frac{1}{\cos\ \theta} + \frac{1}{\cos\ \theta_o}\right]$$

ϕ_o = solar azimuth

ϕ = spacecraft azimuth angle from pixel to sensor (see Figures 2 and 3)

where

$m(\lambda)$ = the refractive index of seawater at λ

$$y = \frac{[m(\lambda)^2 + \cos^2 x - 1]^{1/2}}{m(\lambda)} \tag{11}$$

$$z = [\cos x + ym(\lambda)]^{-2} + [y + m(\lambda) \cos x]^{-2} \tag{12}$$

These equations have been cast in the form of Sturm (1981). The reader should refer to Figures 2 and 3 for proper orientation, as differences in angle-naming convention have been noted in the literature.

The next term in the equation is $S(\lambda,\lambda_o)$ which we shall put aside for the moment.

The next two terms in the equation are derived for λ_o in the same manner as described above for λ. Rationale for determination of λ_o = 670 nm is discussed in the next paragraph.

The last term is $t(\lambda_o)L_W(\lambda_o)$. In order to proceed, the atmospheric correction depends on the quick attenuation in the ocean of radiation at 670 nm (CZCS band 4). Assuming no contaminating source in the water column, such as sediment from the rivers or phytoplankton, the ocean water itself should radiate little at this wavelength. Therefore for clear water $L_W(670) = 0$. (Smith and Wilson (1981) provide an iterative approach to this problem for $L_W(670) \neq 0$.) So if we select 670 nm as λ_o, $t(\lambda_o)L_W(\lambda_o)$ drops out, i.e., all the radiance in this band is due to atmospheric effect (for clear water), and we can solve for $S(\lambda, \lambda_o)$.

So, for CZCS wavelengths 443, 520 and 550 nm:

$$L_W(443) = \frac{L_T(443) - L_R(443) - S(443,670)\,[L_T(670) - L_R(670)]}{t(433)} \tag{13}$$

$$L_W(520) = \frac{L_T(520) - L_R(520) - S(520,670)\,[L_T(670) - L_R(670)]}{t(520)} \tag{14}$$

$$L_W(550) = \frac{L_T(550) - L_R(550) - S(550,670)\,[L_T(670) - L_R(670)]}{t(550)} \tag{15}$$

Note the only unknown term on the right side of Equations 13-15 is $S(\lambda,670)$. To solve for $S(\lambda,670)$ we must select a clear water pixel. These pixels may be assumed to have a known radiance. For clear water pixels with pigment concentrations less than 0.25 mg/m^3, Gordon and Clark (1981) have shown that:

$$L_W(\lambda) = [L_W(\lambda)]_N \cos\theta_o \exp\left[-\frac{\frac{\tau_R}{2} + \tau_{oz}}{\cos\theta_o}\right] \tag{16}$$

where

$[L_W(520)]_N$ = 0.498 mW/cm^2-μm-sr, the normalized water-leaving radiance at 520 nm (16a)

$[L_W(550)]_N$ = 0.30 mW/cm^2-μm-sr, the normalized water-leaving radiance at 550 nm (16b)

$[L_W(670)]_N$ = <0.015 mW/cm^2-μm-sr, the normalized water-leaving radiance at 670 nm (16c)

Thus all the terms except $S(\lambda,670)$ in Equations 14 and 15 are known and the expressions can be solved algebraically for $\varepsilon(\lambda,670)$. $\varepsilon(443,670)$ is solved by extrapolation as it has been shown that $\varepsilon(\lambda,670)$ is a smooth function of n (see below). One solves according to the following equations:

$$\varepsilon(443,670) = [443/670]^{n(443)} \tag{17}$$

where

$$n(443) = 0.5 \left[\frac{\log \varepsilon\ (520,670)}{\log\ (520/670)} + \frac{\log \varepsilon\ (550,670)}{\log\ (550/670)} \right]$$

In practice, either a skilled user will select (based on oceanographic experience) a clear water pixel from a preview image or an automated procedure can be used. One possible automated method is to use a first iteration of ε to derive trial pigment concentrations. In general, the pixel with the lowest pigment value (subject to certain other tests) is acceptable as the clear water pixel. Gordon et al. (1983a) spell out the procedure as follows. Determination of ε's is effected by carrying out the above process using, as a first iteration, $\varepsilon(\lambda_i) = 1$ for i = 1-3. The region of lowest C (pigment concentration) is located using Equation 18, then Equations 4 and 13-17 are solved for ε_{443}, ε_{520}, and ε_{550} using L_T values averaged over a 5 × 5 pixel region to minimize noise. The "region of lowest C" must also meet the test of having a monotonically decreasing sequence $L_{A_{520}}$, $L_{A_{550}}$, and $L_{A_{670}}$. Of these, the region with the highest $L_{A_{670}}$ is selected. This region is used as the clear water calibration area, ε's are derived using Equations 13-17 and processing continues using the bio-optical algorithm throughout the scene.

In summary, the use of clear water pixels as areas of known L_W allows the calculation of the atmospheric parameter ε, so that correct L_W values can be computed throughout the scene without simultaneous in-water radiance measurements.

Once a satisfactory set of ε's is derived, these are applied for each pixel in the scene, and the usual route of extracting $L_W(\lambda)$ from $L_T(\lambda)$ is followed throughout the image, by Equations 13-15, using $S(\lambda,\lambda_o)$ derived from $\varepsilon(\lambda,\lambda_o)$.

Gordon et al. (1983a) give procedures for atmospheric correction in three cases that violate the assumption of a constant aerosol type. The three cases are: variable aerosol over clear water, two distinct aerosol types with the more turbid type overlying at least some clear water, and two distinct aerosol types with the more turbid type not overlying some clear water. The first case is remedied by deriving $n(\lambda)$ at each pixel. The second is mechanistically identical to the usual procedure as described above. The third case can be handled by manually varying values of $n(\lambda)$. This requires somewhat different procedures to accomplish atmospheric correction in at least a semiautomated fashion.

IV. BIO-OPTICAL ALGORITHM

The bio-optical algorithm is a straightforward transformation from water upwelling radiances, L_W, to pigment values (see Clark, 1981). ("Pigment" means chlorophyll and its associated degradation products. The spectral signatures of chlorophyll and its degradation products are indistinguishable by the CZCS.)

Sea-truth data measurements have yielded the following regression equations for conversion from water upwelling radiances to pigment concentration in mg/m^3.

$$\log_{10} C = 0.053 + 1.71 \log_{10} \frac{L_{W_{550}}}{L_{W_{443}}} \tag{18}$$

$$\log_{10} C = 0.522 + 2.44 \log_{10} \frac{L_{W_{550}}}{L_{W_{520}}} \tag{19}$$

Equation 18 is used as the default. If C derived from Equation 18 is more than 1.5 mg/m^3, then C is determined by Equation 19 if it produces C greater than 1.5 mg/m^3. This is because when C is high, absorbance by pigment causes $L_{W_{443}}$ to become too small to be retrieved with sufficient accuracy from $L_{T_{443}}$. The alternative Equation 19 does not use $L_{W_{443}}$.

These coefficients have been tuned to L_W, the water-leaving radiance. The GSFC procedures convert water-leaving radiance (i.e. just above the air-sea interface) to subsurface radiance, L_{ss} (i.e. just below the air-sea interface), by correcting for Fresnel reflectivity losses through the interface $\left(L_{ss} = m^2 L_W(\lambda)/1 - \rho(\theta)\right)$. That algorithm uses different coefficients in Equations 18 and 19, however. According to Gordon (personal communication), there is no significant difference in using the ratios of the L_W's vs the L_{ss}'s.

V. IMPLEMENTATIONS

A. RSMAS

The University of Miami's Rosenstiel School of Marine and Atmospheric Sciences (RSMAS) has implemented a software system for processing CZCS data. General features of this system are described in Brown and Evans (1982). According to Gordon (personal communication) the RSMAS implementation is as described in Gordon et al. (1983a). RSMAS is conducting research on changes in CZCS sensor response, among other things.

B. Dr. J. Mueller, Naval Postgraduate School

Figure 4 is a flow diagram of the Mueller algorithm. Dr. Mueller has given us code for processing a navigated image. References to subroutines are those listed in Figure 4. It may be instructive to consider the modular nature of Mueller's implementation to gain insight into the required processing steps.

In general, this algorithm does not calculate each parameter at each pixel but rather at every 16th pixel ("anchor point" in CZCS terminology). This approach is also mentioned in Gordon et al. (1983a). To provide the parameters for each pixel, gradients are calculated between the anchor points in the x and y directions.

The program MAIN calls some routines particular to the NPS environment. These routines are JOBNAM, FILNAM, RUNLOG, and TOD -- they need not concern us. Another subroutine called by MAIN is GLOAD. GLOAD gets the navigation parameters, sun zenith and azimuth, and spacecraft zenith and azimuth, for the anchor points. These parameters are copied to a direct-access file for later use.

MAIN then calls SETUP. SETUP sets up some arrays and common blocks. It reads in a NAMELIST of parameters for defining a data window, reads the gain, reads the exponent for Equation 17, and reads a threshold for land/cloud flag. One difference between the Mueller and Gordon implementations is that Mueller depends on an estimate of $n(\lambda)$ (see Equation 17) to derive $\varepsilon(\lambda)$, while Gordon uses estimates of ε derived from the aerosol radiances to estimate $n(\lambda)$. This is a conventional rather than a substantive difference. Other parameters set flags for printing some diagnostic output. SETUP calls subroutines ABEND and RUNLOG, both site-specific routines. It also calls three routines, SUNFLX, SETCAL, and OPTICS to read in more coefficients. SUNFLX calculates the F_o' values (see Equation 2 for F_o'). SETCAL reads in calibration coefficients. OPTICS reads in some atmospheric optical coefficients.

The next routine called by MAIN is PROCES, which does line-by-line processing (i.e., it is counting lines). PROCES in turn calls SETBLK (sets up the arrays for interpolation), GETLIN (gets a scanline of data from tape), LINCAL (computes radiances and flags land/cloud pixels), and WRTLIN (outputs a line of data, either radiance data or data flagged as bad).

SETBLK calls GLINES and GREAD, which retrieve a navigation record for the current line from a direct-access file. SETBLK then calls, through ORGVAL, GEOMTY and RADCAL. GEOMTY calculates the angles Ψ_- and Ψ_+ and atmospheric slant paths for later use. RADCAL calculates L_R's and some intermediate parameters for calculating L_W's. SETBLK then calls GRADS, which through XGRAD and YGRAD, fills the interpolation buffers and repeats the GEOMTY and RADCAL calculations for each pixel.

GETLIN reads in a line of data and does some input checking.

LINCAL does the conversion from counts to radiances. First it flags pixels as land/cloud if the band 5 count is greater than a predetermined threshold. The remaining pixels are processed in subroutines PIXCAL, PIXOUT, and CLPIX. PIXCAL derives L_W's and then pigment and k, the diffuse attenuation coefficient. PIXOUT fills a data buffer, including the unprocessed band 6 counts. CLPIX is an alternative output routine for diagnostic purposes.

The fourth subroutine called by PROCES is WRTLIN, which does the physical output of data.

The remaining subroutines in Figure 4 are DIAGNS and FCON. DIAGNS is a routine to dump some diagnostic output if a certain flag is set. FCON is a common block used by many routines.

A few unique features of the Mueller algorithm are its use of bilinear interpolation, the estimate of $n(\lambda)$ rather than ϵ in Equation 17, and the processing of data on a swath basis rather than on subsets of a swath.

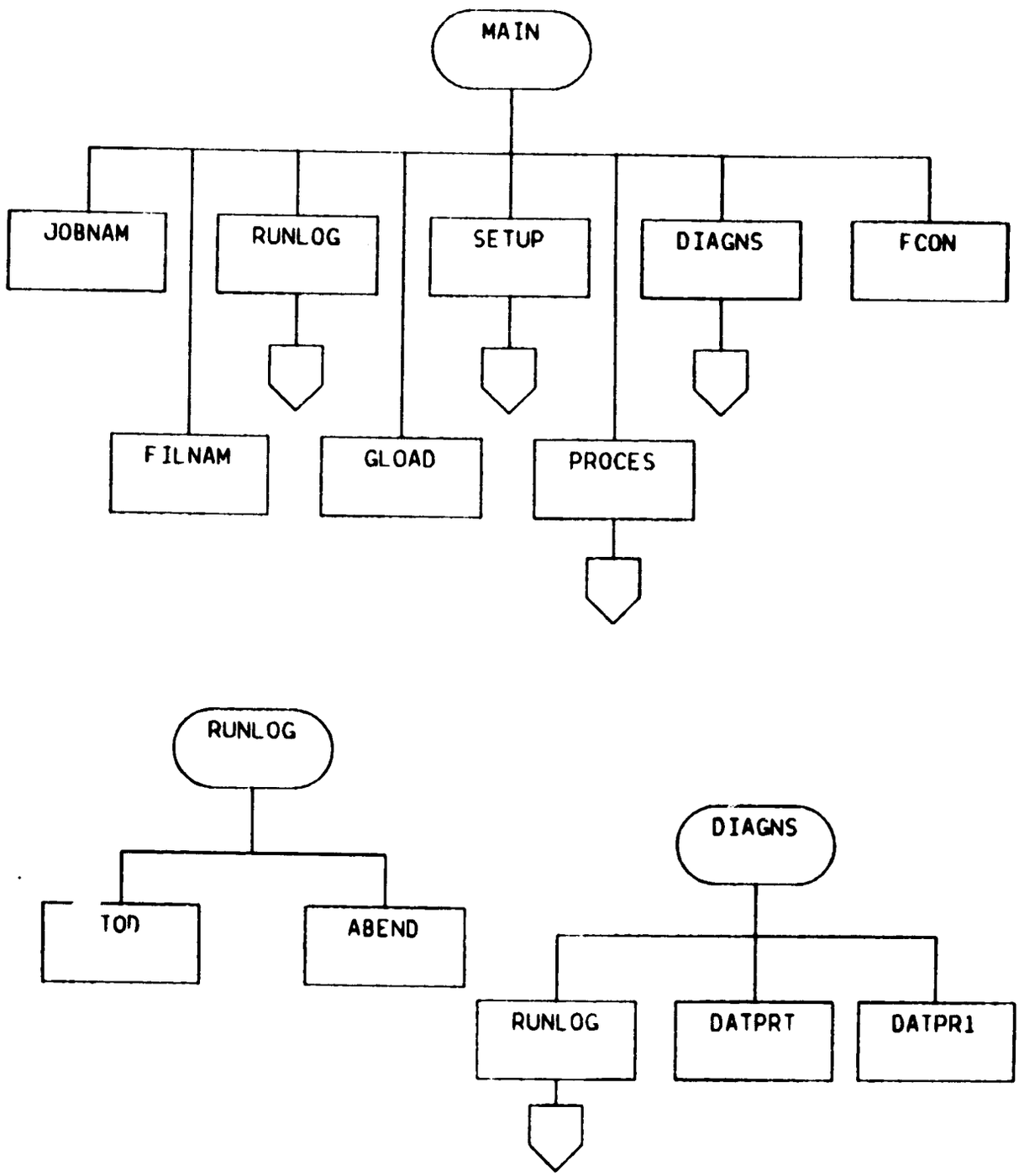

Figure 4. Mueller Processing Flow Diagram (sheet 1 of 3)

SUBROUTINE SETUP CALLS THE FOLLOWING SUBROUTINES

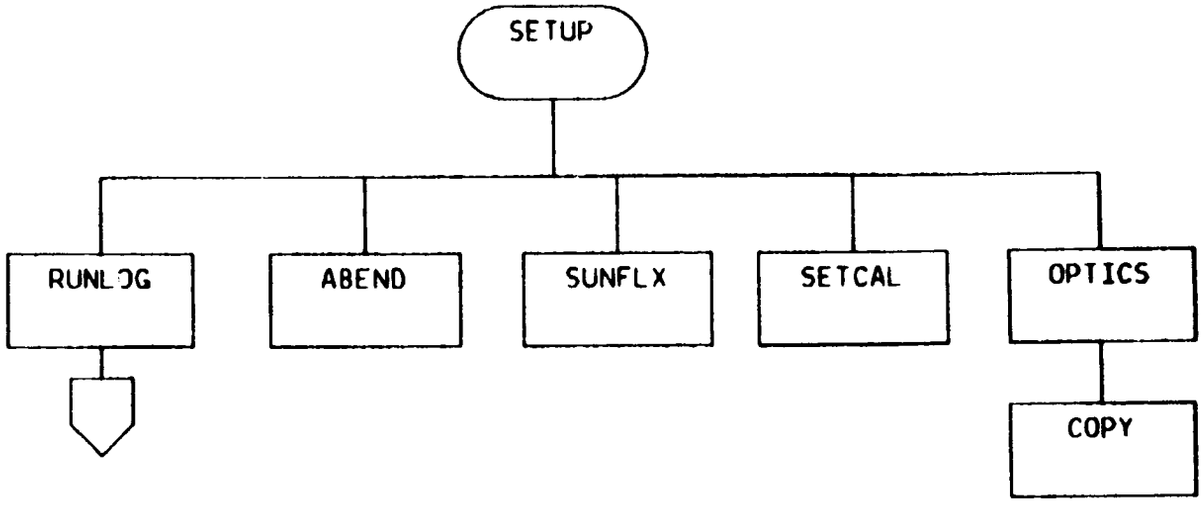

SUBROUTINE PROCES CALLS THE FOLLOWING SUBROUTINES

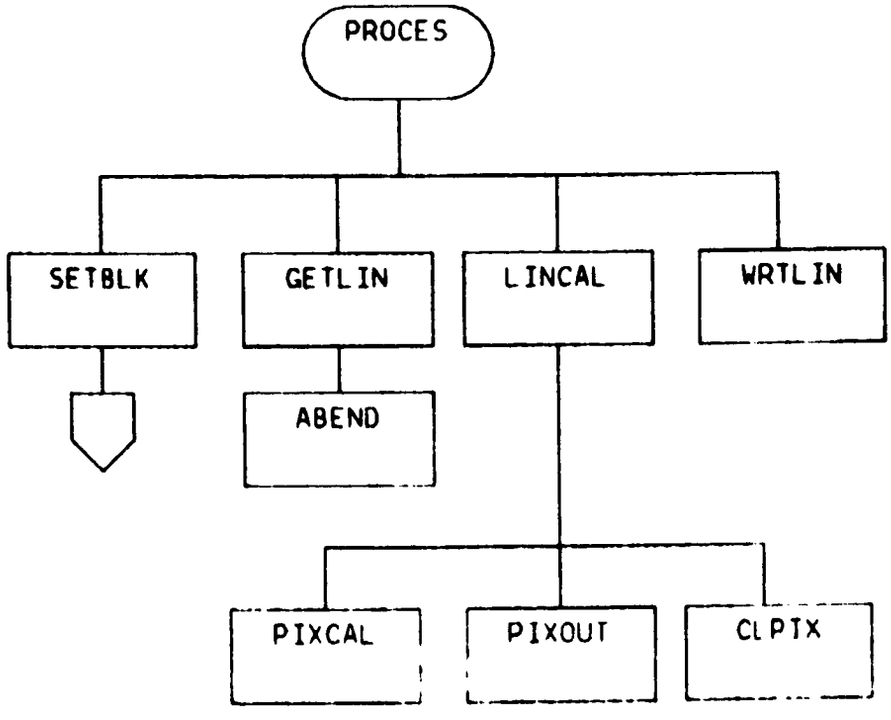

Figure 4. Mueller Processing Flow Diagram (sheet 2 of 3)

SUBROUTINE SETBLK CALLS THE FOLLOWING SUBROUTINES

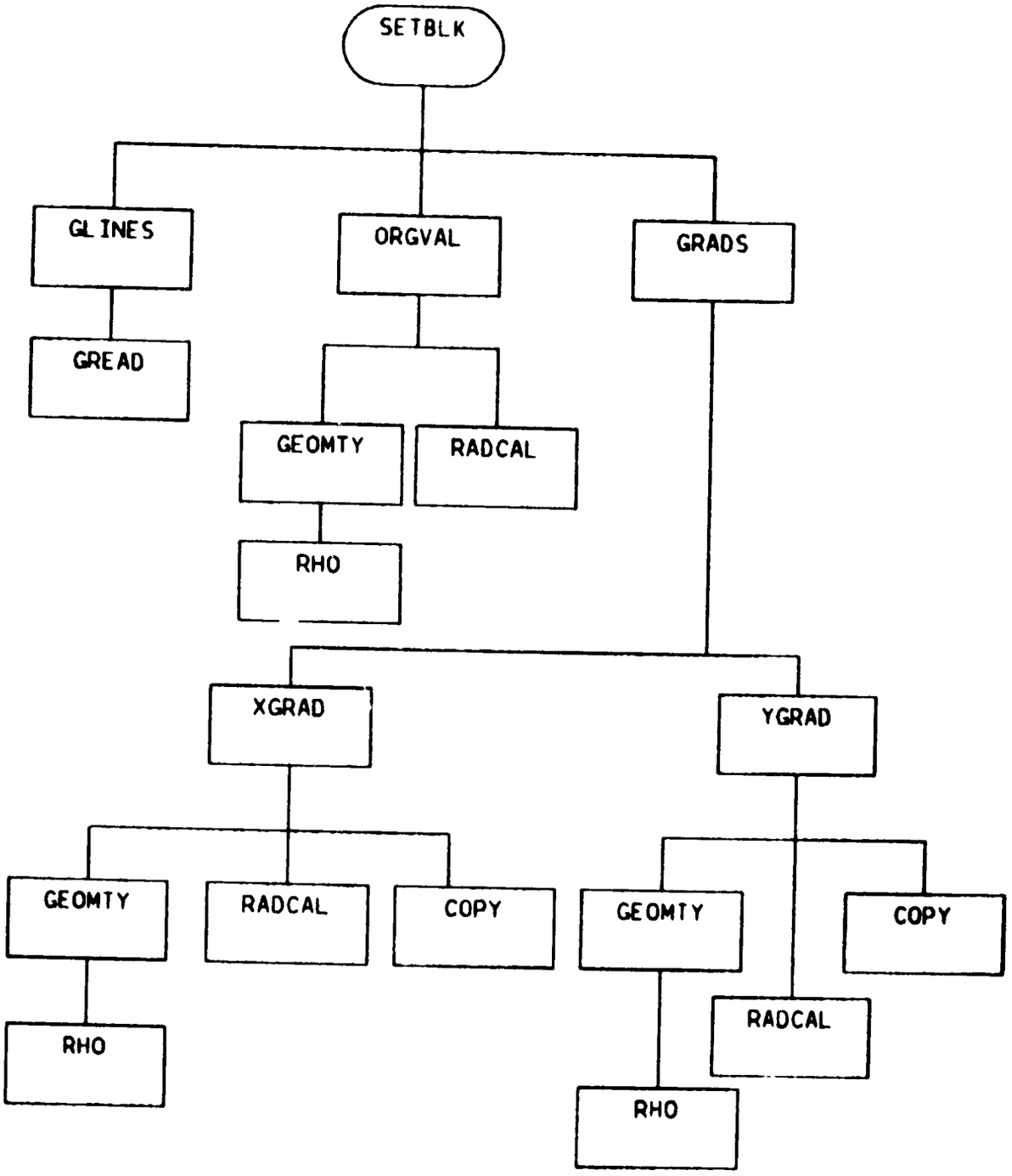

Figure 4. Mueller Processing Flow Diagram (sheet 3 of 3)

C. GSFC Production Algorithm

The GSFC production algorithm is used by NASA to generate products for use by the public. These products are available through NESDIS. They are the closest thing to operational products that exist for CZCS.

The GSFC algorithm depends on partially preprocessed data and ancillary information. This information is contained in the so-called Level-1 tape, which is the input for the GSFC procedures. This information is needed for navigation of the image. Consideration of which data are used by the GSFC algorithm may be instructive.

The first step in the GSFC algorithm is calibration of counts to radiances, including the sensor degradation correction function. This has been presented in Section 2.

The next step is the geometry calculation. This takes place in four stages: scene global, scan line, anchor point, and final geometry calculations. The geometry calculation depends heavily on vector arithmetic for the navigation.

The scene global calculation takes place once per scene. The range over the scene of ephemeris time, sun position, spacecraft position, and Greenwich hour angle are calculated. Ephemeris times are on the Level-1 tape. The sun vector is determined from sun right ascension and declination data on the Level-1 tape.

The scan line stage calculates for each line the ephemeris time, sun position, spacecraft position, and hour angle. These calculations are just interpolations in time of the global parameters calculated above.

The anchor point stage uses some 77 predefined anchor points. The Level-1 tape contains preprocessed latitude/longitude coordinates for these locations. The coordinates are converted to vectors. This stage then computes a spacecraft-to-pixel unit vector for each point.

The final geometry calculation computes for each anchor point the solar zenith angle θ_o, the spacecraft zenith angle θ, the scattering phase angles (for use in deriving Rayleigh radiance), the solar azimuth angle ϕ_o, and the spacecraft azimuth angle ϕ (see Figures 5 through 10). These values can then be linearly interpolated in the direction of scan for the non-anchor point pixels, providing a full set of geometry values for each pixel.

After navigation the procedure is similar to the Gordon algorithm (see Figure 1). Solar and atmospheric constants are derived from NAMELISTs. To derive $\varepsilon(\lambda)$'s, the GSFC algorithm searches alternate pixels on alternate scanlines to locate a likely clear-water area. There are three criteria used to test for acceptable clear-water areas. They are spacecraft and solar zenith angles >0.6 radians, radiance L_T at 670 nm less than 1.4 mW/cm^2-sr-um, and $L_{T_{443}}/[L_{T_{520}} + L_{T_{550}}]$ between 0.9 and 2.0. Then calculation of the clear-water radiance can proceed according to Equations 16-16c and $\varepsilon(\lambda)$ can be derived by Equations 13-15.

One difference between the GSFC and Gordon algorithms is the two coefficients in Equations 16a and 16b. The GSFC algorithm uses 0.495 and 0.280 respectively, rather than Gordon's 0.498 and 0.300. Another slight difference is in the method of calculating Rayleigh radiance. The two methods also differ in selection of a clear-water area. The GSFC algorithm selection examines the calculated sets of ε values. Sets of $\varepsilon(\lambda,\lambda_o)$, with a sequence of $\varepsilon(520,670)$, $\varepsilon(550,670)$, 1 which is not monotonic are excluded as are sets with $\varepsilon(443,670)$ greater than 3.0. Unique to GSFC is the method of choosing $\varepsilon(\lambda,\lambda_o)$. The remaining sets of $\varepsilon(\lambda,\lambda_o)$ are compared, and the set having the lowest $\varepsilon(443,670)/L_T(670)$ is chosen as the best for atmospheric correction.

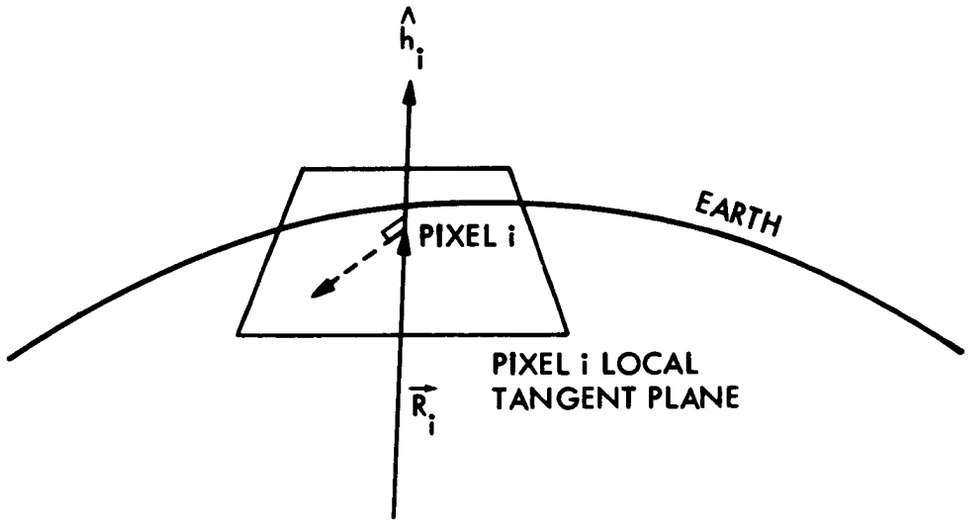

Figure 5. Unit Normal Vector (from GSFC, 1982)

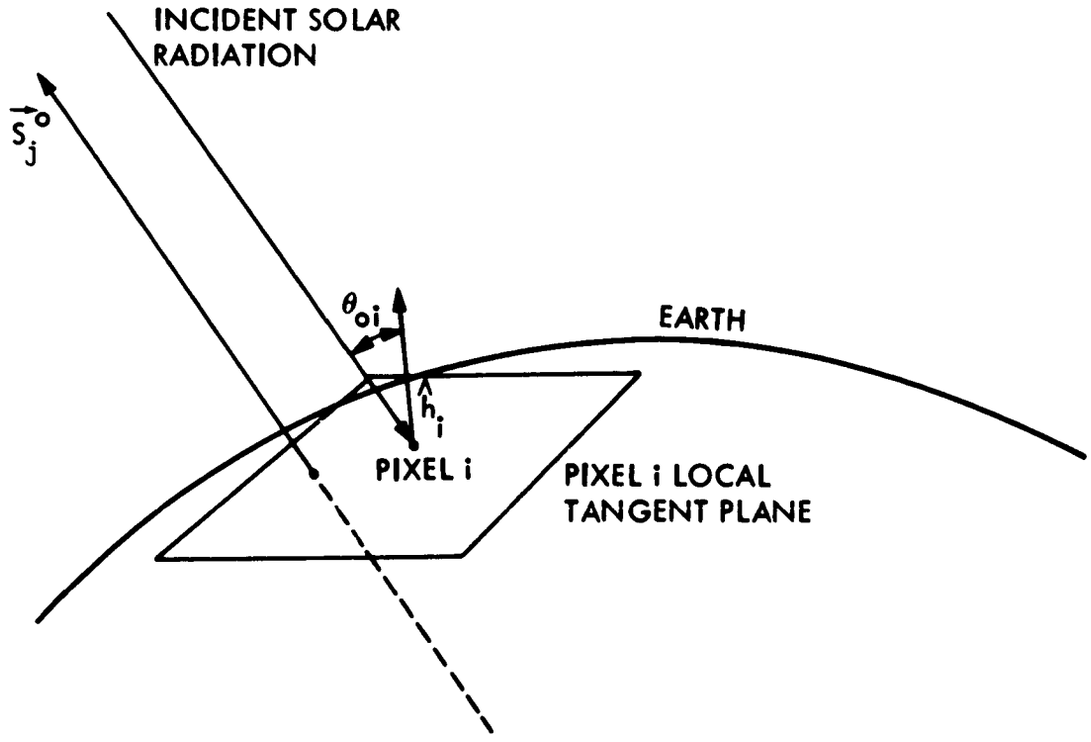

Figure 6. Solar Zenith Angle (from GSFC, 1982)

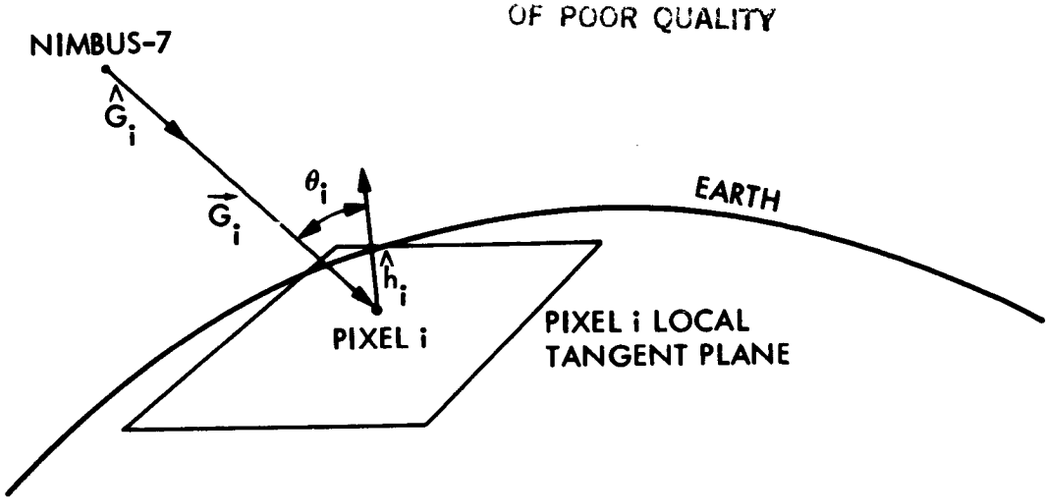

Figure 7. Spacecraft Zenith Angle (from GSFC, 1982)

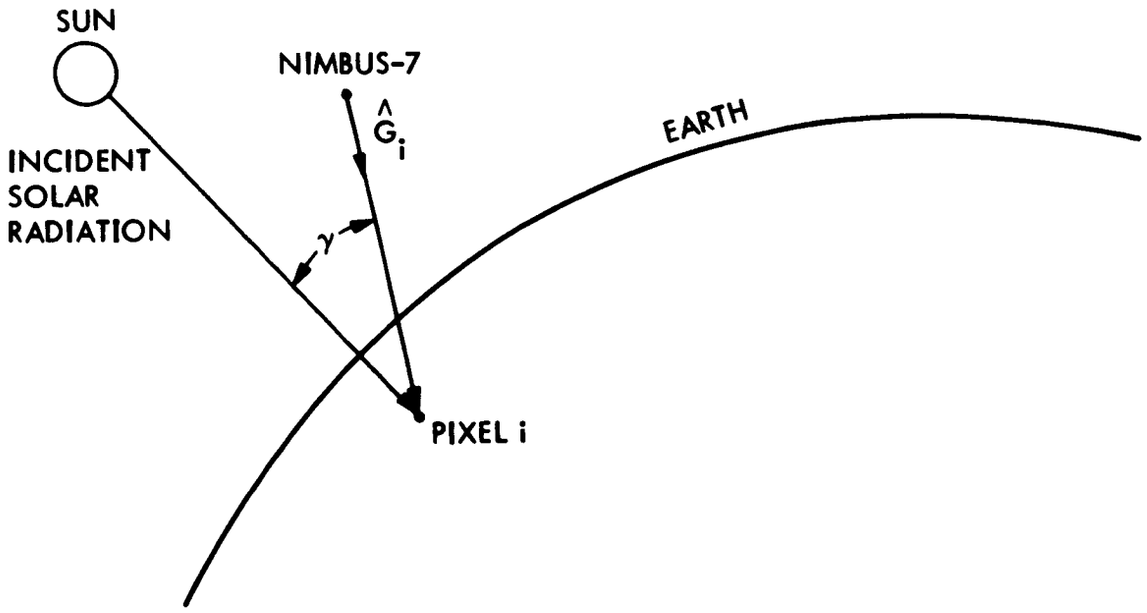

Figure 8. Scattering Phase Angle (from GSFC, 1982)

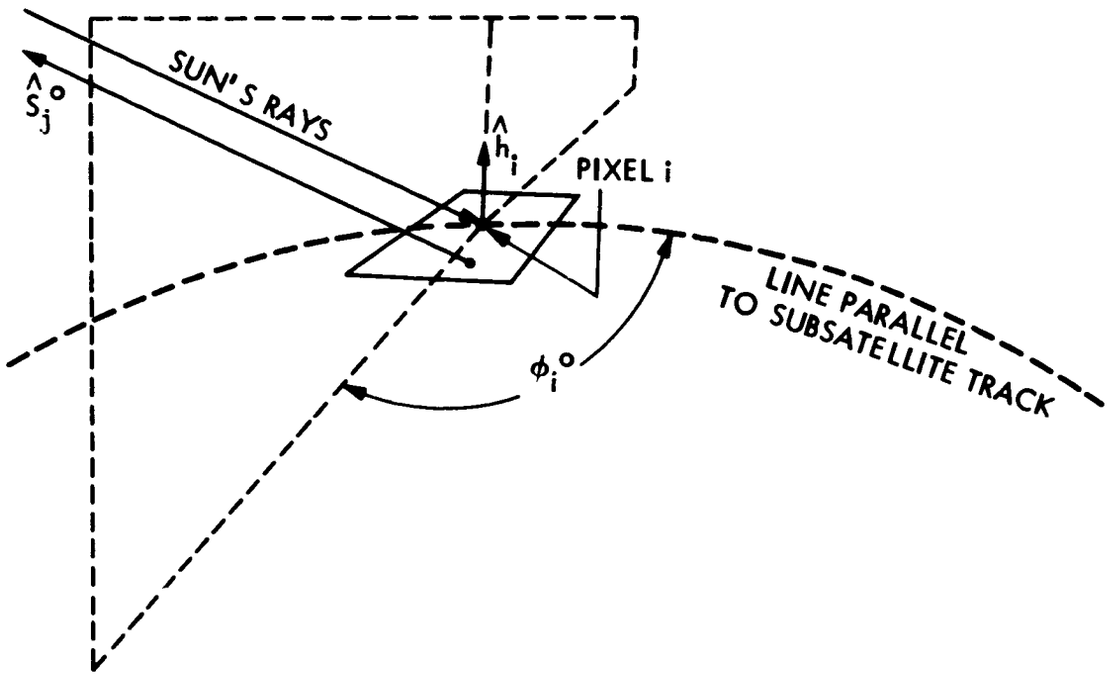

Figure 9. Solar Azimuth Angle (from GSFC, 1982)

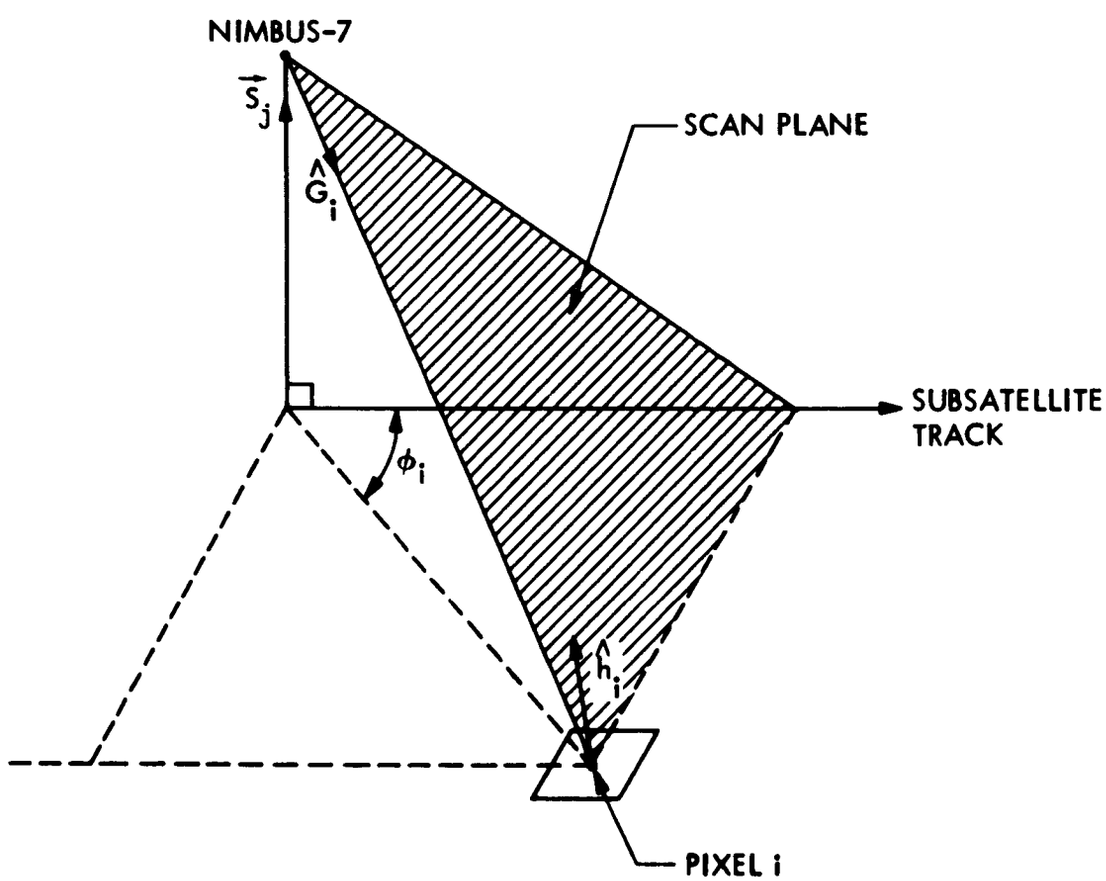

Figure 10. Spacecraft Azimuth Angle (from GSFC, 1982)

VI. REFERENCES

Brown, O.B. and Evans, R.H., 1982. Visible and Infrared Satellite Remote Sensing: A Status Report. Naval Research Reviews, 34 (1), 7-24.

Clark, D.K., 1981. Phytoplankton pigment algorithms for the NIMBUS-7 CZCS, in Oceanography from Space, J.F.R. Gower, ed., Plenum Press, New York, pp. 227-238.

GSFC, COSMIC Software Documentation Volume GSC-12852, COSMIC Data Center, Athens, GA, 1982?

Gordon, H.R., 1981. Reduction in error introduced in the processing of coastal zone color scanner-type imagery resulting from sensor calibration and solar irradiance uncertainty. Applied Optics, 20, 207-210.

Gordon, H.R. and Clark, D.K., 1981. Clear water radiances for atmospheric correction of coastal zone color scanner imagery. Applied Optics, 20, 4175-4180.

Gordon, H.R., Clark, D.K., Brown, J.W., Brown, O.B., Evans, R.H., and Broenkow, W.W., 1983a. Phytoplankton pigment concentrations in the Middle Atlantic Bight: comparisons of ship determinations and CZCS estimates. Applied Optics, 22, 20-36.

Gordon, H.R., Brown, J.W., Brown, O.B., Evans, R.H., and Clark, D.K., 1983b. NIMBUS-7 Coastal Zone Color Scanner (CZCS): Reduction of its radiometric sensitivity with time. Submitted to Applied Optics.

Mueller, J.L., Naval Postgraduate School, Monterey, CA.

OCSWG (Ocean Color Science Working Group), MAREX Report, NASA/GSFC, 1982.

Smith, R.C., and Wilson, W.H., 1981. Ship and satellite bio-optical research in the California Bight, in Oceanography from Space, J.F.R. Gower, ed., Plenum Press, New York, pp. 281-294.

Sturm, B., 1981. The atmospheric correction of remotely sensed data and the quantitative determination of suspended matter in marine water surface layers, in Remote Sensing in Meteorology, Oceanography and Hydrology, A.P. Cracknell, ed., Ellis Horwood Limited, Chichester, England, pp. 163-197.

Viollier, M., 1982. Radiometric calibration of the Coastal Zone Color Scanner on Nimbus 7: a proposed adjustment. Applied Optics, 21, 1142-1145.